Identification of mechanistically distinct inhibitors of HIV-1 reverse transcriptase through fragment screening

Jennifer La[a,b,1], Catherine F. Latham[a,1], Ricky N. Tinetti[a,c], Adam Johnson[a], David Tyssen[a], Kelly D. Huber[d], Nicolas Sluis-Cremer[d], Jamie S. Simpson[b], Stephen J. Headey[b], David K. Chalmers[b], and Gilda Tachedjian[a,c,e,f,2]

[a]Retroviral Biology and Antivirals Laboratory, Centre for Biomedical Research, Burnet Institute, Melbourne, VIC 3004, Australia; [b]Medicinal Chemistry, Monash Institute of Pharmaceutical Sciences, Monash University, Parkville, VIC 3052, Australia; [c]Department of Microbiology, Monash University, Clayton, VIC 3168, Australia; [d]Division of Infectious Diseases, Department of Medicine, University of Pittsburgh School of Medicine, Pittsburgh, PA 15261; [e]Department of Infectious Diseases, Monash University, Melbourne, 3004, Australia; and [f]Department of Microbiology and Immunology, University of Melbourne, Parkville, VIC 3010, Australia

Edited by Stephen P. Goff, Columbia University College of Physicians and Surgeons, New York, NY, and approved April 23, 2015 (received for review December 13, 2014)

Fragment-based screening methods can be used to discover novel active site or allosteric inhibitors for therapeutic intervention. Using saturation transfer difference (STD) NMR and in vitro activity assays, we have identified fragment-sized inhibitors of HIV-1 reverse transcriptase (RT) with distinct chemical scaffolds and mechanisms compared to nonnucleoside RT inhibitors (NNRTIs) and nucleoside/nucleotide RT inhibitors (NRTIs). Three compounds were found to inhibit RNA- and DNA-dependent DNA polymerase activity of HIV-1 RT in the micromolar range while retaining potency against RT variants carrying one of three major NNRTI resistance mutations: K103N, Y181C, or G190A. These compounds also inhibit Moloney murine leukemia virus RT but not the Klenow fragment of *Escherichia coli* DNA polymerase I. Steady-state kinetic analyses demonstrate that one of these fragments is a competitive inhibitor of HIV-1 RT with respect to deoxyribonucleoside triphosphate (dNTP) substrate, whereas a second compound is a competitive inhibitor of RT polymerase activity with respect to the DNA template/primer (T/P), and consequently also inhibits RNase H activity. The dNTP competing RT inhibitor retains activity against the NRTI-resistant mutants K65R and M184V, demonstrating a drug resistance profile distinct from the nucleotide competing RT inhibitors indolopyridone-1 (INDOPY-1) and 4-dimethylamino-6-vinylpyrimidine-1 (DAVP-1). In antiviral assays, the T/P competing compound inhibits HIV-1 replication at a step consistent with an RT inhibitor. Screening of additional structurally related compounds to the three fragments led to the discovery of molecules with improved potency against HIV-1 RT. These fragment inhibitors represent previously unidentified scaffolds for development of novel drugs for HIV-1 prevention or treatment.

HIV | reverse transcriptase | fragment-based drug discovery | allosteric inhibitors | STD-NMR

With an estimated 35.3 million HIV-infected individuals worldwide in 2012 (1), the HIV/AIDS pandemic continues to pose a serious global health threat. Current treatment involves combination antiretroviral therapy (cART), a regimen comprising three or more drugs from at least two drug classes. HIV drug resistance, dosing schedules that reduce patient compliance, and toxicity can limit the effectiveness of cART (2). Additionally, strategies for HIV preexposure prophylaxis that have been approved (i.e., Truvada), or are in development, use existing HIV drugs that could lead to the generation and transmission of drug-resistant strains of HIV and compromise first-line drug regimens (3). Consequently, there is an urgent need for new classes of antiretroviral drugs with novel mechanisms of action for the treatment and prevention of HIV.

HIV reverse transcriptase (RT) plays an essential role in the virus life cycle and was the first successful enzyme target for HIV therapy (4). The HIV-1 RT is a heterodimer composed of 66-kDa (p66) and 51-kDa (p51) polypeptides that converts the single-stranded viral genomic RNA into a double-stranded proviral DNA precursor through RNA- and DNA-dependent polymerase and RNase H enzymatic activities (4). Thirteen of the 26 approved anti-HIV drugs act on HIV-1 RT, and there are ongoing efforts to identify new RT inhibitors (4). Only two classes of drugs targeting this enzyme are in clinical use: nucleoside/nucleotide RT inhibitors (NRTIs) and nonnucleoside RT inhibitors (NNRTIs). NRTIs are prodrugs that structurally mimic the natural substrates of HIV-1 RT, deoxyribonucleoside triphosphates (dNTPs), but normally lack a 3′-hydroxyl group on the ribose sugar, causing chain termination during nucleic acid synthesis (4). NNRTIs are structurally diverse compounds that inhibit DNA polymerization by binding to an allosteric NNRTI binding pocket (NNIBP) in HIV-1 RT (4). The potential to discover new allosteric site inhibitors is supported by the enzymatic activity of HIV-1 RT being critically dependent on its conformational flexibility (5) and the presence of new allosteric pockets in the HIV-1 RT distinct from the NNIBP (6, 7).

Fragment-based drug discovery (FBDD) is a validated drug design strategy, and a successful alternative to traditional high-throughput screening methods (8). The drug vemurafenib, approved by the US Food and Drug Administration in 2011 for the treatment of metastatic melanoma (9), is the first clinical candidate born out of a fragment-screening program. FBDD is a

Significance

In this study, we demonstrate a strategy using a combination of NMR-based binding and functional assays to screen a library of low-molecular-weight compounds known as fragments to identify new drug precursors that target HIV-1 reverse transcriptase (RT). Using this approach, we have discovered three fragments that inhibit HIV-1 RT and clinically relevant drug-resistant mutants. Enzyme assays demonstrate that at least two of these inhibitors are mechanistically distinct from HIV-1 RT drugs used clinically. One of these fragments inhibits HIV-1 replication in cell-based assays. The small size, hydrophilic nature, and excellent ligand efficiency of these fragments make them good starting points for the development of new classes of RT drugs for HIV-1 prevention or treatment.

Author contributions: J.L., C.F.L., N.S.-C., D.K.C., and G.T. designed research; J.L., C.F.L., R.N.T., A.J., D.T., K.D.H., S.J.H., and G.T. performed research; J.L., C.F.L., A.J., D.T., N.S.-C., J.S.S., S.J.H., D.K.C., and G.T. analyzed data; and J.L., C.F.L., D.K.C., and G.T. wrote the paper.

The authors declare no conflict of interest.

This article is a PNAS Direct Submission.

Freely available online through the PNAS open access option.

[1]J.L. and C.F.L. contributed equally to this work.

[2]To whom correspondence should be addressed. Email: gildat@burnet.edu.au.

This article contains supporting information online at www.pnas.org/lookup/suppl/doi:10.1073/pnas.1423900112/-/DCSupplemental.

powerful tool for identifying chemical scaffolds for the development of new drugs and also for locating novel druggable binding sites because the biophysical methods used in hit detection do not require prior knowledge of the potential binding sites or mechanisms of action. Fragments are small compounds with molecular masses typically in the range of 100–250 Da (10) that can be optimized into high-affinity drugs. The low chemical complexity of fragments compared with conventional small-molecule inhibitors reduces the number of compounds required to sample the chemical space efficiently (8); as a result, fragment screens exhibit higher hit rates than conventional small-molecule screens (8).

Due to their small size, fragment hits are typically weak binders with high micromolar to millimolar affinity. Accordingly, highly sensitive biophysical methods are required to detect compound binding to the target protein. Surface plasmon resonance (SPR), ligand-detected NMR spectroscopy, X-ray crystallography, and thermal shift assays are widely used techniques for fragment screening (11). Each technique has its advantages and disadvantages, and a combination of complementary, orthogonal techniques is often used to screen fragment libraries and validate hits (12). Once identified, the screening hits can be ranked using various metrics, including ligand efficiency (13) or the binding efficiency index (BEI) (14), both of which score activity in assays as a function of molecular size.

In this study, we used two complementary methods, saturation transfer difference (STD) NMR and in vitro enzyme inhibition assays, to identify inhibitors of HIV-1 RT that are distinct mechanistically from NRTIs and NNRTIs. Our fragment screen and substructure analysis of one hit identified a total of seven active fragments that are chemically dissimilar to all other known HIV-1 RT inhibitors (Binding DB; www.bindingdb.org) (4, 7, 15), including those HIV-1 RT inhibitors identified in two previously published FBDD programs that used either SPR-based (16) or X-ray crystallography-based (6) screening. Three of the seven scaffolds that we identified have activities consistent with their ability to bind to sites distinct from the NNIBP on the HIV-1 RT, with one of these fragments inhibiting HIV-1 replication in cell culture at the reverse transcription step. Screening of structural analogs of these three scaffolds led to the identification of additional compounds that were more potent inhibitors of HIV-1 RT than the original fragments. These three fragment hits and their more active analogs represent good candidates for structural studies and for the commencement of a medicinal chemistry program to develop highly potent novel inhibitors of HIV-1 RT.

Results

Fragment Screening by STD-NMR and Validation by Recombinant RT Inhibition Assays. We screened 630 fragments from the Maybridge fragment library (average molecular mass of 208 Da) using STD-NMR (17) to identify fragments that bind to His-RT52A (RT52A), an engineered HIV-1 RT construct optimized for high-resolution crystallography (18). The fragments were screened in mixtures of up to five compounds that were designed to preclude signal overlap in such a way that each fragment could be identified by its individual 1D ^{1}H-NMR spectrum. This initial screen identified 84 fragments that bound to RT52A for a hit rate of 13% (Fig. 1*A*), representing a similar hit rate (~17%) reported in a previous FBDD STD-NMR screen with HIV-1 integrase (17).

A fragment-binding event does not necessarily lead to inhibition of enzyme function. To determine which fragments inhibited RT function and to eliminate false-positive results from the STD-NMR screen, the available fragment hits were tested in vitro for inhibition of the RNA-dependent DNA polymerase (RDDP) activity of WT RT from HIV-1 strain LAI [RT (WT)]. Assays were performed under conditions designed to limit fragment aggregation that could lead to nonspecific inhibition of HIV-1 RT activity. Of the 81 fragment hits that were available for testing, 12 demonstrated greater than 50% inhibition of RT (WT) polymerase activity at 0.5 mg/mL (Fig. 1*A*). The 12 fragments were further evaluated in RDDP inhibition assays against RT (WT) and RT52A to generate inhibitory dose–response curves. Six of the top fragment hits (**1**–**6**) (Fig. 1*B*) inhibited the RDDP activity of both RT (WT) and RT52A with IC_{50} values in the micromolar range (Table 1), which is excellent potency for fragments (8). A search for compounds similar to aniline **6** led to the testing of 14 additional compounds for RT inhibitory activity that identified two fragment-sized molecules, nitrobenzene **7** and *p*-hydroxyaniline **8** (Fig. 1*B*), that were more potent inhibitors of RT (WT) and RT52A than the parent compound (Table 1).

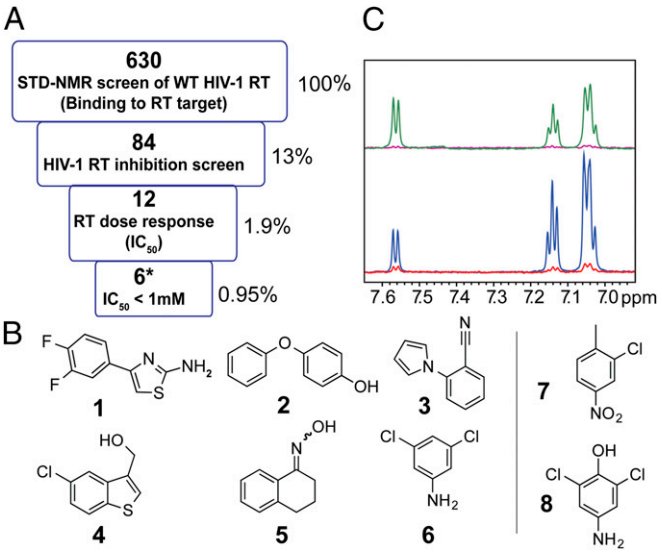

Fig. 1. Overview of fragment library screening and hit validation against HIV-1 RT. (*A*) Fragments were selected at each phase of screening using both binding assays (STD-NMR) and HIV-1 RT inhibition assays, leading to the identification of six fragments with IC_{50} values of <1 mM for RT (WT). (*B*) Chemical structures of eight fragments, including the six fragments from the screen and fragments **7** and **8** that were identified in a substructure search of fragment **6** that inhibited RT (WT). (*C*, *Top*) One-dimensional ^{1}H-NMR STD-NMR spectra of fragment **5** with (green) and without RT (WT) (red). A significant magnetization transfer to the compound is only evident in the presence of RT. (*C*, *Bottom*) CPMG-NMR spectra of fragment **5** with (red) and without RT (WT) (blue). Increased T2 relaxation causing a large decrease in the compounds' peak heights is evident in the presence of RT.

Dynamic light scattering was used to screen for aggregates of particle size ≥30 nm at different fragment concentrations under RT assay conditions (Table S1). This assay was used to eliminate nitrile **3** (Fig. 1*B*) from the study. A nonaggregating concentration range was determined for the other seven fragments (Table S1), which was used for all subsequent assay conditions. Binding to RT (WT) by the seven remaining hits, including oxime **5** (Fig. 1*C*) and fragments **1**, **2**, **4**, and **6**–**8**, was confirmed as individual compounds by STD-NMR (Fig. S1) and by Carr–Purcell–Meiboom–Gill (CPMG) NMR (Fig. S2), a method that exploits the different correlation times of small and large molecules to detect ligand binding. The BEI values (14) of fragments **5**–**8** for RT (WT) are in a range similar to the optimized NNRTIs nevirapine (NVP) and efavirenz (EFV) (Table 1), suggesting that they are good starting points for elaboration into more potent inhibitors.

Chemical Similarity Search of HIV-1 RT Inhibitor Database Reveals Previously Unidentified Structures of Hits. To determine that the hits represented new chemical scaffolds for HIV-1 RT inhibitors, a Tanimoto similarity search was performed to compare our seven hits with the 1,531 RT inhibitors recorded in the Binding DB (4, 15, 19, 20) and with fragments identified in previous FBDD screens for HIV-1 RT inhibitors: the nine fragments reported by Bauman et al. (6) and the bromoindanone NNRTI identified by Geitmann et al. (16). A Tanimoto score of 80% or greater is generally regarded as high structural similarity. The seven HIV-1 RT inhibiting fragment hits identified in our screen

Table 1. Inhibition of polymerase activity of WT and drug-resistant HIV-1 RT

Compound	Molecular mass, Da	RDDP IC_{50} ± SE,* μM		DDDP IC_{50} ± SE,* μM				LogP†	BEI (mol·L^{-1}·kDa^{-1})‡
		RT (WT)	RT52A	RT (WT)	RT (K103N)	RT (Y181C)	RT (G190A)		
1	212	613 ± 197	120 ± 26	758 ± 81	—	—	—	2.13	15
2	186	747 ± 148	127 ± 18	617 ± 44	—	—	—	2.56	17
3	168	67 ± 12§	57 ± 6§	—	—	—	—	1.79	—
4	199	556 ± 27	31 ± 6	259 ± 34	382 ± 120 (1.5)¶	129 ± 29 (0.5)	333 ± 93 (1.3)	2.2	18
5	161	436 ± 27	22 ± 12	222 ± 12	149 ± 36 (0.7)	119 ± 15 (0.5)**	227 ± 36 (1.0)	2.7	23
6	162	295 ± 31	42 ± 5	247 ± 25	489 ± 97 (2.0)**	317 ± 66 (1.3)	668 ± 205 (2.7)**	1.98	22
7	172	129 ± 10	28 ± 24	11 ± 2	51 ± 5 (4.6)**	13 ± 5 (1.2)	23 ± 3 (2.1)**	3.08	29
8	178	194 ± 16	24 ± 12	222 ± 21	128 ± 18 (0.6)**	194 ± 23 (0.9)	191 ± 34 (0.9)	1.75	20
EFV		7 ± 2#	4 ± 1#	0.017 ± 0.008‖	0.3 ± 0.2 (18)**	0.02 ± 0.02 (1.4)	0.05 ± 0.02 (2.9)		25
NVP		—	—	0.44 ± 0.08‖	35 ± 12 (80)**	37 ± 10 (84)**	50 ± 5 (114)**		24

*IC_{50} ± SE for RDDP activity from $n = 3$ assays and DDDP activity from $n = 4$ assays for all except RT (WT), where data are from $n = 5$ independent assays.
†LogP values were calculated using Instant JChem, version 5.12.0 (ChemAxon, www.chemaxon.com).
‡BEI was calculated using DDDP IC_{50} values with the equation $-\log_{10}[IC_{50}(mol/L)]$/molecular mass (kDa).
¶Fold change was calculated by the ratio of RT-mutant IC_{50} to WT-RT IC_{50} values.
§Aggregates were observed using dynamic light scattering at these concentrations.
#$n = 5$, where n is the number of independent assays.
‖$n = 3$, where n is the number of independent assays.
**There was a significant difference between IC_{50} values for RT mutants compared with RT (WT): $P < 0.05$.

demonstrated no more than 42% similarity to any of the compounds from previous screens or in the compiled database. This low similarity indicates that the chemical structures of our active hits have not been previously reported to inhibit HIV-1 RT.

HIV-1 RT DNA-Dependent DNA Polymerase Inhibitory Activity of Fragments Against Recombinant WT and NNRTI Drug-Resistant HIV-1 RT Mutants. Having progressed through the initial screens, fragments **1**, **2**, and **4**–**8** were evaluated for inhibition of HIV-1 RT DNA-dependent DNA polymerase (DDDP) activity using activated calf thymus (ACT) DNA as the heteropolymeric template/primer (T/P). All seven hits had IC_{50} values in the micromolar range (Table 1). The DDDP activities against RT (WT) were similar to the measured RDDP activities, except for nitrobenzene **7**, where 12-fold greater potency was observed for DDDP activity. The five hits with the most potent RDDP and DDDP activities against RT (WT) (fragments **4**–**8**) were examined for their ability to inhibit three clinically relevant NNRTI-resistant mutants (RT_{K103N}, RT_{Y181C}, and RT_{G190A}) (21) using DDDP assays (Table 1). All five fragments inhibited the three RT mutants with IC_{50} values in the micromolar range. Fragments **6** and **7** were twofold and 4.6-fold less potent against the RT_{K103N} mutant ($P < 0.05$, $n \geq 4$) compared with RT (WT), where n is the number of independent assays, and 2.7-fold and 2.1-fold less potent against the RT_{G190A} mutant (both $P < 0.05$, $n \geq 4$). The significant decrease in potency of fragments **6** and **7** against these two NNRTI drug-resistant mutants suggests that they potentially bind at or proximal to the NNIBP. Conversely, fragments **4**, **5**, and **8** inhibited all three NNRTI-resistant mutants with similar or increased potency compared with RT (WT). Fragment **8** was almost twofold more potent against the RT_{K103N} mutant compared with RT (WT) ($P < 0.05$, $n = 4$), whereas fragments **4** and **5** were similarly potent against RT_{K103N} and RT (WT). Oxime **5** was the only compound with significantly different potency against the Y181C mutation ($P < 0.05$, $n = 4$), which demonstrated twofold hypersusceptibility to RT_{Y181C} compared with RT (WT) (Table 1). The three RT mutants demonstrated the expected NVP and EFV drug susceptibility profiles (Table 1). The potency of fragments **4**, **5**, and **8** was not adversely affected by the NNIBP mutations tested, suggesting that they bind at the NNIBP but are unaffected by Y181C, K103N, and G190A or that they bind at another site that is unperturbed by these mutations. We then used a Hill plot analysis of the DDDP activity data for fragments **4**, **5**, and **8** to determine the number of functional binding sites on RT (WT) that lead to inhibition of DDDP activity. We included 2′,3′-dideoxy CTP (ddCTP) and EFV as control compounds that are known to inhibit HIV-1 RT by binding to a single site on the enzyme (4). The Hill coefficients for fragments **4**, **5**, and **8** were close to or equal to 1.0, similar to those Hill coefficients obtained for ddCTP and EFV (Fig. S3), suggesting noncooperative binding. Although this analysis cannot exclude the possibility that multiple fragments bind to RT (WT), our data do indicate that only one of the binding interactions for each fragment is responsible for inhibiting HIV-1 RT function.

Fragments 5 and 8 Inhibit HIV-1 RT by Distinct Mechanisms from HIV-1 Drugs in Clinical Use. We investigated the mechanism of action of fragments **4**, **5**, and **8** that retained potency against NNRTI-resistant RT, using steady-state DDDP kinetic assays and Dixon plot analysis (22) to determine whether the compounds act by competing with RT dNTP substrate or a heteropolymeric double-stranded ACT-DNA T/P. Oxime **5** was identified as a competitive inhibitor of HIV-1 RT with respect to dNTP; with a K_i value of 220 ± 74 μM ($n = 4$) (Fig. 2*A*). Supporting the Dixon plot analysis, we found that the IC_{50} value of fragment **5** increased with increasing dNTP concentrations (Table S2). Competition with dNTPs suggests that oxime **5** binds at or near the polymerase active site, possibly to the allosteric binding pocket described for nucleotide-competing RT inhibitors (NcRTIs) (7) or another allosteric site.

p-Hydroxyaniline **8** was shown to compete with the DNA T/P substrate using steady-state kinetic DDDP inhibition assays (Fig. 2*B*; $K_i = 30 \pm 9$ μM, $n = 4$) and by a gel mobility shift assay that tested for inhibition of T/P binding to HIV-1 RT (Fig. 2 *C* and *D*; $IC_{50} = 92.9 \pm 1.1$ μM, $n = 4$). In addition, the IC_{50} of *p*-hydroxyaniline **8** increased with increasing T/P concentration, consistent with an RT inhibitor that competes with T/P (Table S3). It is possible that a fragment could inhibit DNA binding by intercalating the DNA T/P. However, this proposition is considered unlikely in the case of *p*-hydroxyaniline **8** because the STD-NMR and CPMG-NMR experiments show direct binding of the fragment to HIV-1 RT (Figs. S1 and S2).

To characterize the dNTP-competing oxime **5** further, we tested its activity against two NRTI-resistant mutants of HIV-1 RT, RT_{M184V} and RT_{K65R} (Table S4), to determine if it has a similar profile to the NcRTIs, 4-dimethylamino-6-vinylpyrimidine-1 (DAVP-1) (20) and indolopyridone-1 (INDOPY-1) (23). The T/P-competing *p*-hydroxyaniline **8** was also evaluated. Oxime **5** demonstrated twofold increased potency for RT_{K65R} but no change in potency for RT_{M184V} (Table S4). This profile is partially similar to INDOPY-1, which is

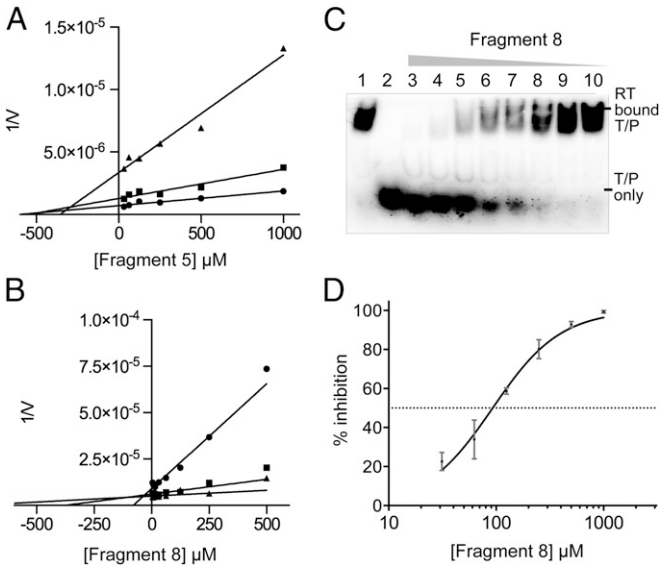

Fig. 2. Fragments **5** and **8** inhibit HIV-1 RT with mechanisms of action distinct from NRTIs and NNRTIs. (*A*) Dixon plot analyses of HIV-1 RT DDDP inhibition by oxime **5** from assays performed with nonsaturating concentrations of dNTP substrate (●, 5 μM dNTP; ■, 10 μM dNTP; ▲, 20 μM dNTP) and a saturating concentration of T/P (100 ng/μL ACT-DNA). (*B*) Dixon analysis of HIV-1 RT DDDP inhibition by *p*-hydroxyaniline **8** from assays performed with nonsaturating concentrations of T/P (●, 5 ng/μL ACT-DNA; ■, 10 ng/μL ACT-DNA; ▲, 20 ng/μL ACT-DNA) and a saturating concentration of dNTP (50 μM dNTP). For *A* and *B*, the Dixon method was performed by plotting fragment concentration vs. the inverse of the reaction velocity (1/*V*) of the DDDP reaction. The $-K_i$ of the fragment is equal to the *x* intercept, calculated by linear regression. Lines that intersect above the *x* axis represent competitive inhibitors with respect to the dNTP or ACT T/P substrate. Representative Dixon plots from $n = 4$ independent assays are shown. (*C*) Gel mobility shift assay to show competition between *p*-hydroxyaniline **8** with DNA T/P binding to HIV-1 RT. Lanes 1 and 2 denote no drug and no RT, respectively. Lanes 3–10 are assays performed with RT in the presence of 1,000, 500, 250, 125, 62.5, 31.3, 15.1, and 7.6 μM fragment **8**. (*D*) Quantitation of data from gel mobility shift assays with fragment **8** from $n = 4$ independent assays. Error bars denote SEM.

also more potent against RT_{K65R} but is fivefold less potent for RT_{M184V} (23). Hydroxyaniline **8** retained potency against both mutants (Table S4). Taken together with their activity against NNRTI-resistant RT (Table 1), these data indicate that oxime **5** and *p*-hydroxyaniline **8** have resistance profiles distinct from the NcRTIs INDOPY-1 and DAVP-1.

Inhibition of HIV-1 RT RNase H Activity by *p*-Hydroxyaniline 8. Fragments **4**, **5**, and **8** were evaluated for their ability to inhibit the RNase H activity of HIV-1 RT. *p*-Hydroxyaniline **8** inhibited HIV-1 RT RNase H activity with an IC_{50} of 173 ± 3 μM ($n = 4$), whereas benzothiophene **4** and oxime **5** lacked inhibitory activity (Fig. S4). Because *p*-hydroxyaniline **8** was shown to bind with similar affinity to RT (WT) by STD-NMR (Fig. S1) and CPMG-NMR (Fig. S2) in the presence or absence of EDTA, it is unlikely that inhibition of RNase H activity was due to coordination of divalent cations at the RNase H active site, a common mechanism of RNase H inhibitors (4). The inhibition of RNase H activity by *p*-hydroxyaniline **8** further distinguishes its inhibitory profile from conventional NNRTIs. This assay demonstrates that *p*-hydroxyaniline **8** inhibits not only the RDDP and DDDP activities of RT (WT) and RT mutants but also the RNase H activity of the enzyme.

Activity of Fragments 4, 5, and 8 Against Moloney Murine Leukemia Virus RT and DNA Polymerases. We investigated the RT specificity of the three fragment hits (**4**, **5**, and **8**) by evaluating their inhibitory activity against four other DNA polymerases: a retroviral RT, Moloney murine leukemia virus (MoMLV) RT; the human DNA polymerase β (POLB) and/or polymerase γ (POLG) (Table S5); and a bacterial DNA polymerase *Escherichia coli* Klenow fragment. Benzothiophene **4** and *p*-hydroxyaniline **8** demonstrated similar potency against MoMLV RT compared with HIV-1 RT. In contrast, oxime **5** was 4.4-fold ($P < 0.05$, $n \geq 3$) less potent against MoMLV RT compared with HIV-1 RT (Table S5). Because NNRTIs inhibit HIV-1 RT but not other RT enzymes (24), the ability of fragments **4**, **5**, and **8** to inhibit MoMLV RT activity suggests that they are unlikely to target the NNIBP. None of the fragments inhibited the bacterial Klenow DNA polymerase within the assessable concentration range ($IC_{50} > 5$ mM for **4**, **5**, and **8**; $n = 4$), which was inhibited by foscarnet (IC_{50} of 1.7 ± 0.2 mM, $n = 4$). Fragments **4** and **5** were fourfold to greater than ninefold less potent inhibitors of human POLB and POLG compared with WT HIV-1 RT, whereas fragment **8** had similar potency against POLB and was more potent against POLG (Table S5). Although *p*-hydroxyaniline **8** inhibits POLB and POLG, the lack of activity of this hit and fragments **4** and **5** against *E. coli* Klenow fragment indicates that they do not broadly inhibit DNA polymerase enzymes through a general or nonspecific mechanism.

***p*-Hydroxyaniline 8 Displays Anti–HIV-1 Activity in Cell Culture.** Because several fragments displayed HIV-1 RT inhibition, we investigated whether any of these compounds had anti–HIV-1 activity in cell culture. One of these compounds, *p*-hydroxyaniline **8**, inhibited HIV-1 replication at noncytotoxic levels with an EC_{50} of 20 ± 6 μM ($n = 4$) (Fig. S5*A*) and a selectivity index of 8. To confirm that the HIV-1 inhibitory activity of *p*-hydroxyaniline **8** was consistent with targeting the reverse transcription step in the viral life cycle, we performed a time-of-addition assay, where the fragment was added at fixed time points after viral infection (Fig. S5*B*). Known inhibitors of HIV-1 attachment/entry (the bicyclam AMD3100, a CXCR4 antagonist), reverse transcription (NVP), and integration (raltegravir) steps were tested in parallel. Our data demonstrate that *p*-hydroxyaniline **8** has a similar inhibition profile to NVP (Fig. S5*B*), which strongly suggests that *p*-hydroxyaniline **8** acts at the reverse transcription stage of the HIV-1 life cycle.

Identification of Additional Compounds Structurally Related to Fragments 4, 5, and 8 That Are More Potent and Specific Inhibitors of HIV-1 RT Compared with POLB and POLG. We evaluated a total of 49 compounds related to fragments **4** ($n = 17$), **5** ($n = 18$), and **8** ($n = 14$) for inhibition of RT (WT) DDDP activity (Table S5). Of these compounds, 24%, 22%, and 64% of the compounds (Fig. S6) inhibited HIV-1 RT, including compounds **9**, **13**, and **17**, which had greater potency (3.2- to 5.3-fold) than the parent fragments **4**, **5**, and **8** (Table S5). Compounds **9**, **13**, and **17** were tested for activity against human POLB and POLG (Table S5). Based on fold differences between IC_{50} values, compounds **9** and **13** demonstrated greater specificity for HIV-1 RT compared with POLB (>27- and 48-fold, respectively) and POLG (12- and 13-fold, respectively) than their original counterparts fragment **4** (6.9-fold for POLB and 3.9-fold for POLG) and fragment **5** (greater than ninefold for both POLB and POLG). Similarly, compound **17** was more specific for HIV-1 RT compared with POLB (>29-fold) and POLG (2.4-fold) compared with the original fragment **8**, which had similar and greater potency for POLB and POLG, respectively, compared with HIV-1 RT. When compounds **9**, **13**, and **17** were assessed for inhibition of MoMLV RT, a similar pattern of inhibition to the original fragments was observed except for compound **9**, which showed dramatically greater potency for HIV-1 RT (14.9-fold) compared with the parent fragment **4** (1.4-fold), indicating greater specificity for HIV-1 RT compared with the MoMLV RT enzyme (Table S5).

Discussion

Using an FBDD screening cascade (Fig. 1*A*), we successfully identified seven fragments with previously unidentified structures that inhibit HIV-1 RT and some clinically relevant NNRTI- and NRTI-resistant mutants with RDDP and DDDP inhibitory activity

in the micromolar range. The STD-NMR screen identified fragments with a hit rate of 13%, which significantly reduced the number of fragments for testing in the secondary functional screen for RT inhibitory activity. Enzyme kinetic assays revealed that oxime **5** and *p*-hydroxyaniline **8** act competitively with respect to the dNTP and nucleic acid substrates of HIV-1 RT, respectively. Collectively, our data indicate that compounds **4**, **5**, and **8** may be targeting sites distinct from the HIV-1 RT NNIBP because they maintain or have increased potency against NNRTI-resistant forms of HIV-1 RT and inhibited MoMLV RT.

Two groups have previously reported FBDD initiatives targeting HIV-1 RT. Geitmann et al. (16) used SPR to screen 1,040 fragments to identify compounds that bind to the NNIBP. They identified a bromoindanone scaffold that bound to WT HIV-1 RT with a K_d of 270 μM. In follow-up RT polymerization activity assays, this compound was fourfold to 10-fold less potent against three clinically relevant NNRTI drug-resistant RT mutants. Bauman et al. (6) used high-throughput X-ray crystallography fragment screening to probe HIV-1 RT for novel allosteric binding sites. Nine fragments were reported that bound to seven distinct sites. Three of these pockets were found to be functionally significant using HIV-1 RT inhibition assays, although detailed mechanistic studies, including the ability of fragments to inhibit drug-resistant RT or inhibit HIV-1 replication, were not performed. In contrast to previous FBDD screens for HIV-1 RT inhibitors, we used STD-NMR to detect binding of fragments to HIV-1 RT. An advantage of this method over X-ray crystallography and SPR is the ability to monitor the interaction between HIV-1 RT and the fragments free in solution, allowing for maximum conformational flexibility of the protein. STD-NMR allows rapid screening of compounds as mixtures, which is not possible for RT functional assays, especially given the high concentrations of each fragment required for testing. Although one caveat of fragment screening using STD-NMR is that it can have a high rate of false-positive results (25), we overcame this issue by using functional assays to validate and determine the inhibitory activity of our hits.

p-Hydroxyaniline **8** inhibits RDDP, DDDP, and RNase H activity, and it competes with the T/P substrate of HIV-1 RT. Importantly, low micromolar concentrations of *p*-hydroxyaniline **8** inhibit HIV-1 replication in cell culture with a time-of-addition profile consistent with an RT inhibitor. The chemical structure of *p*-hydroxyaniline **8** differs from aniline **6** by a *para*-hydroxyl group, and this difference has marked effects on the capability of aniline **6** to inhibit RNase H activity and to inhibit polymerase activity of the NNRTI-resistant mutants K103N and G190A. The ability of *p*-hydroxyaniline **8** to compete with the comparatively large DNA T/P molecule suggests that it may bind either to location(s) along the DNA-binding groove to block T/P binding or to an allosteric site on RT that induces a conformational change that perturbs the T/P binding interaction. Known inhibitors of RNase H generally coordinate divalent cations at the RNase H active site and lack specificity for HIV RT (4). Allosteric HIV-1 RT RNase H inhibitors that also disrupt polymerization activity have been reported, such as *N*-(4-tert-butylbenzoyl)-2-hydroxy-1-naphthaldehyde hydrazone and its analogs (26, 27). The multiple modes of inhibition shown for *p*-hydroxyaniline **8** similarly suggest that one or more of its mechanisms are allosteric. Large and hydrophobic T/P-competing molecules that block HIV-1 RT function, such as SY-3E4 (494 Da) (28), KM-1 (823 Da) (29), and APEX57219 (422 Da) (15), are also known; however, their size makes them undesirable as drug development leads. In contrast, *p*-hydroxyaniline **8** demonstrates exceptional potency for its size, suggesting it may show promise as a candidate for further development.

Anilines (e.g., *p*-hydroxyaniline **8**) and related compounds are known as potentially problematic false-positive compounds and have been identified as pan assay interference compounds (PAINS) (30). Frequently, this problematic activity is a result of redox activity, through oxidation to the corresponding quinonoid compounds and the formation of covalent adducts with proteins. We considered the possibility that compound **8** might be oxidized under assay conditions to a quinone that could then react to form a covalent protein adduct, but we were unable to find evidence to support this proposition. To reduce the potential for oxidation, functional assay conditions were performed under reducing conditions (i.e., 1 mM DTT), making the conversion of *p*-hydroxyaniline **8** to oxidized species less likely. Freshly prepared *p*-hydroxyaniline **8** in DMSO had similar RT inhibitory activity to stocks stored for several months. A comparison of *p*-hydroxyaniline **8** with the corresponding *p*-quinone, 2,6-dichlorobenzoquinone (2,6-DC), in parallel assays showed that 2,6-DC inhibits both HIV-1 RT (DDDP activity) and Klenow DNA polymerase with IC_{50} values of <4 μM and 72 ± 41 μM, respectively. In comparison, *p*-hydroxyaniline **8** inhibits HIV-1 RT DDDP activity with an IC_{50} value of 156 ± 28 μM but displays little, if any, inhibitory activity against Klenow DNA polymerase (IC_{50} > 5 mM, n = 4) discrediting a nonspecific DNA polymerase mechanism. Critically, trichloroaniline **17**, which is structurally very similar to fragment **8** but cannot form quinonoid oxidation products, also inhibits HIV-1 RT DDDP activity (Table S5) by competing with T/P, as determined using the gel mobility shift assay (774 ± 26 μM, n = 3), and inhibits HIV-1 replication in TZM-bl cells at noncytotoxic concentrations [EC_{50} of 10 ± 3 μM, and a 50% cytotoxic concentration (CC_{50}) of 59 ± 11 μM, n = 3]. Although these data do not clear *p*-hydroxyaniline **8** of problematic compound behavior, they demonstrate there is scope for further development of this compound class through less reactive compounds.

The HIV-1 RT inhibitory fragments **4**, **5**, and **8** did not inhibit Klenow DNA polymerase, suggesting they are unlikely to be exerting their effect by a nonspecific mechanism. This inhibitory specificity is also supported by the finding that fragments **4** and **5** and their analogs, compounds **9** and **13**, that lacked activity against POLB and POLG. Although fragment **8** inhibits POLB and POLG, its more potent HIV-1 RT inhibitory analog, compound **17**, was relatively less active against these host DNA polymerases, indicating the potential for engineering more potent and HIV-1 RT-specific molecules through FBDD. In contrast, fragments **4**, **5**, and **8** and analogs **13** and **17** tended to have similar potency for HIV-1 and MoMLV RT. Although the sequence similarity between HIV-1 RT and MoMLV RT is low, ranging from 6% in the connection domain to 25% in the fingers and palm subdomains, both viral RTs have similar folding arrangements in their polymerase domains (31). The conformational landscape of the binding sites may therefore be very similar. The ability of fragment **5** to inhibit MoMLV RT contrasts with INDOPY-1, which lacks activity against a murine retroviral RT (23), suggesting that this fragment binds to a site distinct from this NcRTI. Moreover, compounds **4**, **5**, and **8** are unlikely to target the NNIBP because NNRTIs are usually highly specific for the HIV-1 RT and do not inhibit MoMLV RT activity (24).

The spectrum of activity against RT mutants provides some insights into their potential modes of action. Oxime **5** is a competitive inhibitor of HIV-1 RT with respect to the dNTP substrate. Oxime **5** retains similar inhibitory activity against the NcRTI- and NNRTI-resistant mutants tested and does not structurally resemble the dNTPs with which it competes. The crystal structure of the NcRTI DAVP-1 complexed with RT has revealed a discrete binding pocket that is proximal to the polymerase active site located in a hinge region at the interface between the p66 palm and the p51 thumb subdomains (7). The exact binding site of INDOPY-1, which preferentially binds to the binary RT–T/P complex, is unknown (7). Although NNRTIs have recently been shown to prevent dNTP binding to the HIV-1 RT using thermodynamic (32) and single-molecule fluorescence-based assays (33), no studies have shown that NNRTIs compete with dNTP using enzyme kinetic assays as performed in this study. Our data suggest that oxime **5** is of the NcRTI class, but its activity against NNRTI- and NRTI-resistant RT indicates different drug resistance profiles to INDOPY-1 and DAVP-1. The activity profiles presented in this study for fragments **4**, **5**, and **8**, provide strong evidence that they bind to sites distinct from the

NNIBP. Despite our efforts using NMR experiments designed to test this hypothesis directly, high-resolution X-ray crystallography–based structural studies will be required to elucidate the exact binding sites of these fragments and/or their analogs.

Using two-stage screening of a fragment library, we have identified structurally unique compounds that bind and inhibit HIV-1 RT, with our top three hits demonstrating favorable binding efficiencies and lipophilicity indices (Table 1). Extensive characterization of fragments **4**, **5**, and **8** confirmed that oxime **5** and *p*-hydroxyaniline **8** have mechanisms of action distinct from drugs currently in clinical use. We have shown that these three fragments are excellent starting scaffolds for building larger and more potent specific lead compounds. In this regard, our analysis of a small subset of structurally related compounds demonstrates that many are active against HIV-1 RT (Fig. S6 and Table S5) and that the core scaffolds of fragments **4**, **5**, and **8** can be functionalized at several positions for future optimization. Our findings have strong potential to lead to much needed new classes of HIV-1 RT drugs to target resistant RT mutants effectively for HIV prevention or therapy.

Materials and Methods

Fragment Library, Substructure Search, and Antiretroviral Drugs. Details of the origin and verification of the 630 fragments in the initial screen, substructure analysis, and follow-up screen are described in *SI Materials and Methods*.

RT Expression and Purification. HIV-1 RT (WT) protein and HIV-1 RT variant proteins containing one of the K103N, Y181C, G190A, M184V, or K65R mutations were expressed as an N-terminal hexahistidine fusion protein and purified as described (34). MoMLV RT, Klenow DNA polymerase, and human POLB and POLG were purchased from Life Technologies, Promega, and BPS Bioscience, respectively.

RDDP and DDDP Inhibition Assays. Inhibition of HIV-1 RT RDDP was performed using the polyrAoligodT T/P, and HIV-1 RT DDDP, MoMLV RT, Klenow polymerase, and human POLB and POLG assays were performed using ACT-DNA T/P as described in *SI Materials and Methods*. Fragment DDDP inhibition data were plotted using the Hill equation (35). Steady-state kinetic assays, with varying heteropolymeric T/P or dNTP concentrations, were performed as described in *SI Materials and Methods*.

RNase H Inhibition Assay. Assays were performed using a ^{32}P-labeled 35-nt RNA template (5′-AGAAUGGAAAAUCUCUAGCAGUGGCGCCCGAACAG-3′) annealed to a 26-nt DNA primer (5′-CCTGTTCGGGCGCCACTGCTAGAGAT-3′) using a denaturing gel-based assay (36) and the FRET-based RNase H cleavage assay (37) as described in *SI Materials and Methods*.

Detailed descriptions of STD-NMR screening and CPMG-NMR testing of individual fragments, gel mobility shift assays assessing competition with T/P for binding to HIV-1 RT, HIV-1 inhibition assays in TZM-bl cells, and RT52A (18) protein production from pRT52A-tobacco etch virus are provided in *SI Materials and Methods*.

ACKNOWLEDGMENTS. We thank Martin Scanlon for providing the fragment library, advice on STD-NMR, and reading the manuscript. We thank the NIH AIDS Research and Reference Reagent Program, Division of AIDS, National Institute of Allergy and Infectious Diseases, NIH, for providing MT-2, 293T, and TZM-bl cells and the antiviral drugs AMD3100, INDOPY-1, NVP, EFV, and raltegravir. We acknowledge the contribution to this work of the Victorian Operational Infrastructure Support Program received by the Burnet Institute. This work was supported by the National Health and Medical Research Council of Australia (NHMRC) (Grant 1064900) and the Percy Baxter Charitable Trust, Perpetual Trustees (to C.F.L. and G.T.). G.T. was supported by NHMRC Senior Research Fellowship 543105, and J.L. was supported by a Monash University Postgraduate Scholarship. N.S.-C. was supported by Grant R01GM068406 from the US NIH.

1. UNAIDS (2013) UNAIDS report on the global AIDS epidemic 2013. Available at www.unaids.org/sites/default/files/media_asset/UNAIDS_Global_Report_2013_en_1.pdf. Accessed May 5, 2015.
2. Tsibris AM, Hirsch MS (2010) Antiretroviral therapy in the clinic. *J Virol* 84(11):5458–5464.
3. Gupta RK, et al. (2013) Oral antiretroviral drugs as public health tools for HIV prevention: Global implications for adherence, drug resistance, and the success of HIV treatment programs. *J Infect Dis* 207(Suppl 2):S101–S106.
4. Esposito F, Corona A, Tramontano E (2012) HIV-1 reverse transcriptase still remains a new drug target: Structure, function, classical inhibitors, and new inhibitors with innovative mechanisms of actions. *Mol Biol Int* 2012:586401.
5. Bahar I, Erman B, Jernigan RL, Atilgan AR, Covell DG (1999) Collective motions in HIV-1 reverse transcriptase: Examination of flexibility and enzyme function. *J Mol Biol* 285(3):1023–1037.
6. Bauman JD, et al. (2013) Detecting allosteric sites of HIV-1 reverse transcriptase by X-ray crystallographic fragment screening. *J Med Chem* 56(7):2738–2746.
7. Freisz S, et al. (2010) Crystal structure of HIV-1 reverse transcriptase bound to a non-nucleoside inhibitor with a novel mechanism of action. *Angew Chem Int Ed Engl* 49(10):1805–1808.
8. Hajduk PJ, Greer J (2007) A decade of fragment-based drug design: Strategic advances and lessons learned. *Nat Rev Drug Discov* 6(3):211–219.
9. Tsai J, et al. (2008) Discovery of a selective inhibitor of oncogenic B-Raf kinase with potent antimelanoma activity. *Proc Natl Acad Sci USA* 105(8):3041–3046.
10. Congreve M, Carr R, Murray C, Jhoti H (2003) A 'rule of three' for fragment-based lead discovery? *Drug Discov Today* 8(19):876–877.
11. Meiby E, et al. (2013) Fragment screening by weak affinity chromatography: Comparison with established techniques for screening against HSP90. *Anal Chem* 85(14):6756–6766.
12. Silvestre HL, Blundell TL, Abell C, Ciulli A (2013) Integrated biophysical approach to fragment screening and validation for fragment-based lead discovery. *Proc Natl Acad Sci USA* 110(32):12984–12989.
13. Hopkins AL, Groom CR, Alex A (2004) Ligand efficiency: A useful metric for lead selection. *Drug Discov Today* 9(10):430–431.
14. Abad-Zapatero C, Metz JT (2005) Ligand efficiency indices as guideposts for drug discovery. *Drug Discov Today* 10(7):464–469.
15. Sheen CW, Alptürk O, Sluis-Cremer N (2014) Novel high-throughput screen identifies an HIV-1 reverse transcriptase inhibitor with a unique mechanism of action. *Biochem J* 462(3):425–432.
16. Geitmann M, et al. (2011) Identification of a novel scaffold for allosteric inhibition of wild type and drug resistant HIV-1 reverse transcriptase by fragment library screening. *J Med Chem* 54(3):699–708.
17. Wielens J, et al. (2013) Parallel screening of low molecular weight fragment libraries: Do differences in methodology affect hit identification? *J Biomol Screen* 18(2):147–159.
18. Bauman JD, et al. (2008) Crystal engineering of HIV-1 reverse transcriptase for structure-based drug design. *Nucleic Acids Res* 36(15):5083–5092.
19. Rajotte D, et al. (2013) Identification and characterization of a novel HIV-1 nucleotide-competing reverse transcriptase inhibitor series. *Antimicrob Agents Chemother* 57(6):2712–2718.
20. Maga G, et al. (2007) Discovery of non-nucleoside inhibitors of HIV-1 reverse transcriptase competing with the nucleotide substrate. *Angew Chem Int Ed Engl* 46(11):1810–1813.
21. Wensing AM, et al. (2014) 2014 Update of the drug resistance mutations in HIV-1. *Top Antivir Med* 22(3):642–650.
22. Dixon M (1953) The determination of enzyme inhibitor constants. *Biochem J* 55(1):170–171.
23. Jochmans D, et al. (2006) Indolopyridones inhibit human immunodeficiency virus reverse transcriptase with a novel mechanism of action. *J Virol* 80(24):12283–12292.
24. Yuasa S, et al. (1993) Selective and synergistic inhibition of human immunodeficiency virus type 1 reverse transcriptase by a non-nucleoside inhibitor, MKC-442. *Mol Pharmacol* 44(4):895–900.
25. Dalvit C (2009) NMR methods in fragment screening: Theory and a comparison with other biophysical techniques. *Drug Discov Today* 14(21-22):1051–1057.
26. Borkow G, et al. (1997) Inhibition of the ribonuclease H and DNA polymerase activities of HIV-1 reverse transcriptase by N-(4-tert-butylbenzoyl)-2-hydroxy-1-naphthaldehyde hydrazone. *Biochemistry* 36(11):3179–3185.
27. Felts AK, et al. (2011) Identification of alternative binding sites for inhibitors of HIV-1 ribonuclease H through comparative analysis of virtual enrichment studies. *J Chem Inf Model* 51(8):1986–1998.
28. Yamazaki S, et al. (2007) Aptamer displacement identifies alternative small-molecule target sites that escape viral resistance. *Chem Biol* 14(7):804–812.
29. Wang LZ, Kenyon GL, Johnson KA (2004) Novel mechanism of inhibition of HIV-1 reverse transcriptase by a new non-nucleoside analog, KM-1. *J Biol Chem* 279(37):38424–38432.
30. Baell JB, Ferrins L, Falk H, Nikolakopoulos G (2013) PAINS: Relevance to tool compound discovery and fragment-based screening. *Aust J Chem* 66(12):1483–1494.
31. Coté ML, Roth MJ (2008) Murine leukemia virus reverse transcriptase: Structural comparison with HIV-1 reverse transcriptase. *Virus Res* 134(1-2):186–202.
32. Bec G, et al. (2013) Thermodynamics of HIV-1 reverse transcriptase in action elucidates the mechanism of action of non-nucleoside inhibitors. *J Am Chem Soc* 135(26):9743–9752.
33. Schauer GD, Huber KD, Leuba SH, Sluis-Cremer N (2014) Mechanism of allosteric inhibition of HIV-1 reverse transcriptase revealed by single-molecule and ensemble fluorescence. *Nucleic Acids Res* 42(18):11687–11696.
34. Yap SH, et al. (2007) N348I in the connection domain of HIV-1 reverse transcriptase confers zidovudine and nevirapine resistance. *PLoS Med* 4(12):e335.
35. Hill AV (1910) The possible effect of the aggregation of the molecules of haemoglobin on its oxygen dissociation curve. *J Physiol* 40:iv–vii.
36. Radzio J, Sluis-Cremer N (2008) Efavirenz accelerates HIV-1 reverse transcriptase ribonuclease H cleavage, leading to diminished zidovudine excision. *Mol Pharmacol* 73(2):601–606.
37. Parniak MA, Min KL, Budihas SR, Le Grice SF, Beutler JA (2003) A fluorescence-based high-throughput screening assay for inhibitors of human immunodeficiency virus-1 reverse transcriptase-associated ribonuclease H activity. *Anal Biochem* 322(1):33–39.